NUMERICAL SIMULATION OF EXPERIMENTS WITH COMMERCIAL EXPLOSIVES

Y.A. Aminov, N.S. Eskov, G.V. Kovalenko, Y.R. Nikitenko, V.I. Volkov,

V.P. Voronina

Russian Federal Nuclear Center – Zababakhin Institute of Technical Physics (RFNC-VNIITF)

Snezhinsk, Russia

The presentation discusses numerical modeling of experiments [1] aimed at testing the properties of the commercial explosive PZhV-20U. Calculations were made with MACH code [2] that models complex 2D flows with account for physical and chemical transformations. A unique approach was used to describe experiments aimed to characterize:

- detonation velocity versus diameter for cylindrical explosive charges;
- the expansion of detonation-propelled copper sheathes; and
- explosive sensitivity to shock.

The calculations demonstrate good agreement with experimental results.

COMPUTATIONAL SETUP

Equations of state for inert materials

For inert materials, we used the Mie-Gruneisen equation of state

$$P = P_x + \gamma\rho(E - E_x), \quad P_x = \frac{\rho_0 C_0^2}{n}\left(\delta^n - 1\right).$$

Here P is pressure, E is specific internal energy, P_x and E_x are cold components, ρ_0 and C_0 are, respectively, density and sound speed for non-compressed material, $\delta=\rho/\rho_{0k}$, ρ_{0k} is crystalline density, and γ and n are constants. Table 1 contains values used for these parameters.

Table 1. Parameters of the equation of state for inert materials

Material	ρ_0, g/cm^3	ρ_{0k}, g/cm^3	C_0, km/s	γ	n
Fluoroplastic	2.19	2.19	1.7	1.883	6.4
Copper	8.9	8.937	3.60	2.67	6.0

Equation of state for the PZhV-20U explosive

For the non-reacting explosive, we used the Mie-Gruneisen equation with the following parameters:

ρ_{0k}=1.7975 g/cm^3; C_0=3 km/s; n=6.35; γ=1.2366.

These values were obtained previously.

Figure 1 shows experimental and calculated Hugoniots for the PZhV-20U explosive of initial densities ρ_0=1.15 g/cm^3 and ρ_0=1.70 g/cm^3. The theoretical equation of state is quite accurate for the calculation that considers explosive decomposition kinetics because minor differences from experimental results can be adjusted with properly selected free parameters in the kinetic equation.

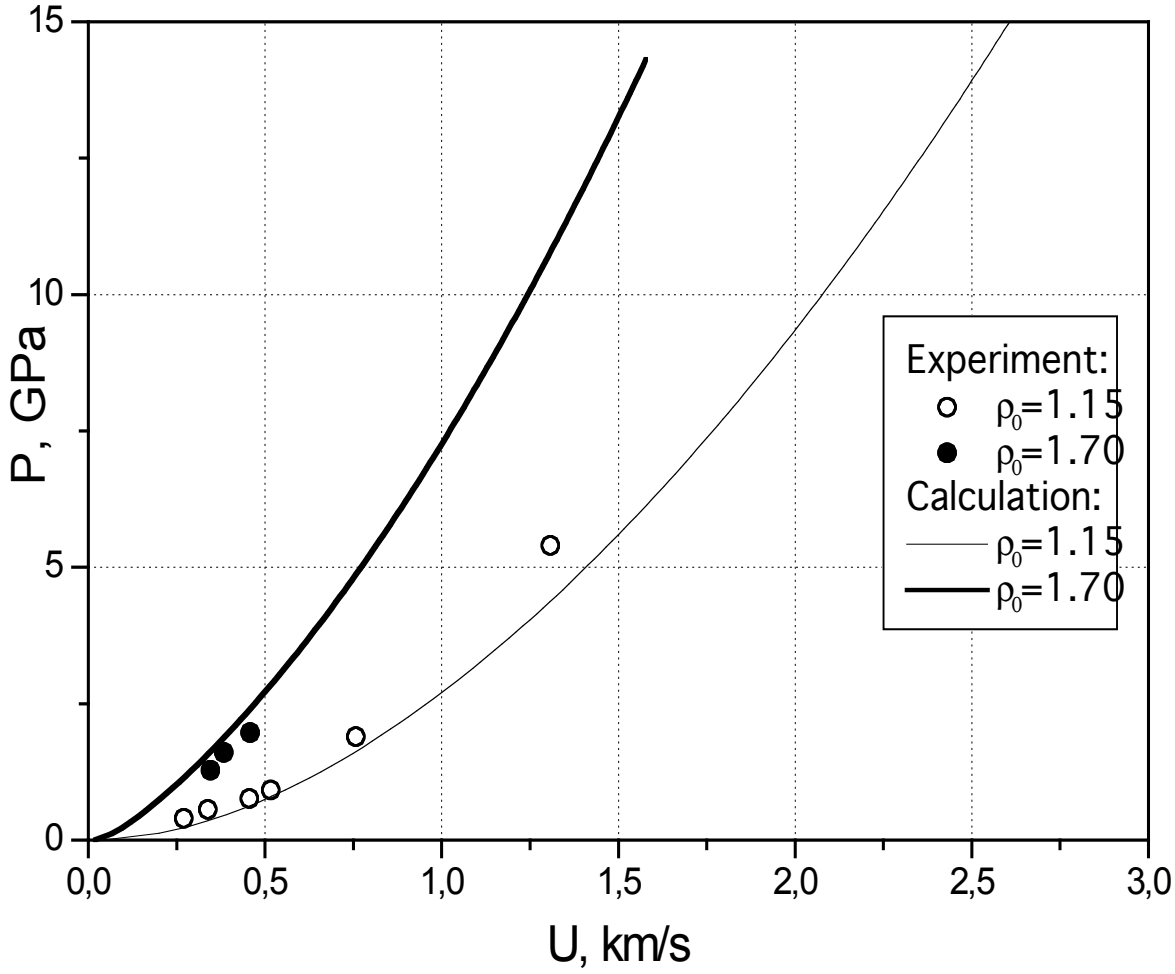

Fig. 1. Experimental and calculated Hugoniots for the PZhV-20U explosive

For detonation products, we used the equation of state by V.F. Kuropatenko [3], based on generalized relationships obtained through the analysis of experimental data for a great number of single- and multi-component explosives. It can be used for any explosive by defining 4 parameters: ρ_{0k}, ρ_0, D_{0k} and α. Our calculations were made with D_{0k}=5.6 km/s and α=0.35. For the initial density

ρ_0=1.2 g/cm^3, the calculated detonation velocity and Chapman-Jouguet pressure are, respectively, D_{CJ}=4.86 km/s and P_{CJ}=8.1 GPa.

Explosive decomposition model

Decomposition of the PZV-20U explosive was described using a two-stage semiempirical model of detonation macrokinetics, developed at RFNC-VNIITF [4]. The model is based on the "hot spots" hypothesis proved in numerous experiments with heterogeneous explosives. The kinetic equation is written in the form

$$\frac{d\xi}{dt} = \begin{cases} -W \cdot \dfrac{\rho_{HE}}{\rho_{0k}^{1/3} \cdot \rho_{DP}^{2/3}} \cdot \left(\dfrac{1-\xi}{\theta}\right)^{2/3} \cdot \exp\left(-E_a / 3E_t^*\right) U(\sigma), & \dfrac{\theta \cdot \xi}{\rho_{HE}} > \dfrac{1-\xi}{\rho_{DP}}; \\ -W \cdot \left(\dfrac{\rho_{HE}}{\rho_{0k}}\right)^{1/3} \cdot \xi^{2/3} \cdot \exp\left(-E_a / 3E_t^*\right) U(\sigma), & \dfrac{\theta \cdot \xi}{\rho_{HE}} \le \dfrac{1-\xi}{\rho_{DP}}. \end{cases}$$

$$W = W_0\left(\alpha + \frac{\beta}{1+\exp(\lambda(\mu-\xi))}\right),$$

$$U(\sigma) = arctg\left(a\sigma + b\sigma^m\right).$$

Here ξ is explosive mass concentration; ρ_{0k} is explosive crystalline density; σ=P/P_{CJ}; P_{CJ} is Chapman-Jouguet pressure; E_a is the effective activation energy defining the minimum pressure under which the explosive begins to decompose; E_t^* is the thermal specific internal energy of the explosive on the wave front; $U(\sigma)$ is a dimensionless burning front "velocity" which is a step function of pressure. This relationship allows the adequate description of main features in the decomposition of heterogeneous explosives: hot spot combustion under low pressures and homogeneous combustion at high pressures. The first phase of the model describes the combustion of hot spots and the second one treats surface combustion after the hot spots have merged. The factor $\exp(E_a / 3E_t^*)$ relates to the number of hot spots initiated by the shock wave propagating in the explosive.

The kinetics model parameters used in the calculations are presented in Table 2.

Table 2. Kinetics model parameters

W_0, μs^{-1}	E_a, kJ/g	a	b	m	θ	α	β	λ	μ
11.37	0.15	0.108	1.1	4.6	0.25	0.125	0.875	35	0.8

The use of the selected function $W(\xi)$ of decomposition depth as a unique factor results in the fact that the rate of explosive decomposition during the second phase is much lower than during the first phase. In the physical context this reflects the presence of two components – trotyl and ammonium nitrate – that significantly differ in combustion rate.

Figure 2 shows the pressure profile obtained in calculation with the above equations of state and allowance for decomposition kinetics for PZhV-20U stationary detonation. At the end of the reaction region the profile is very quiet; the pressure reduces by only 1 GPa per 2 mm. This results

from the slow decomposition of the main PZhV-20U component - ammonium nitrate that makes the detonation of this explosive markedly "non-ideal". That is why it is difficult to experimentally measure the time when the release of energy ends and identify the reaction zone followed by rarefaction. This may lead to large errors in the width of the reaction zone. What also adds to the error of measurements made with built-in transducers is the inevitable distortion of the hydrodynamic flow. As seen from Fig. 2, the calculated width of the PZhV-20U reaction zone formally occupies ~5 mm.

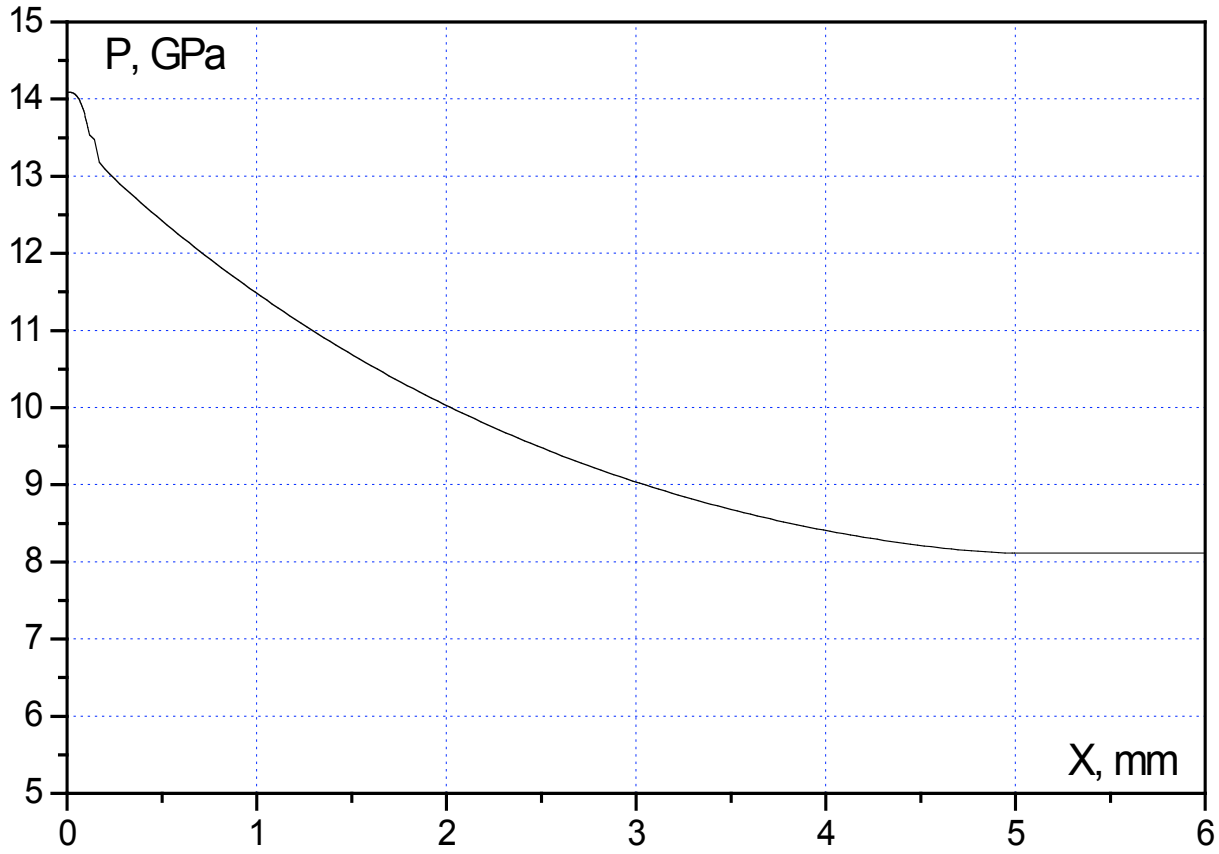

Fig. 2. Calculated pressure profile for PZhV-20U stationary detonation

Non-sheathed cylindrical charges

Calculations were done to study the evolution and propagation of detonation waves in non-sheathed cylindrical PZhV-20U charges of different diameters. The computational setup corresponds to the actual experimental assembly. A cylindrical PZhV-20U charge of the initial density ρ_0=1.2 g/cm^3 is adjacent to a primer of the same diameter. The primer is a strong 20 mm thick explosive in which we calculated ideal detonation, using the equation of state by V.F. Kuropatenko with the parameters ρ_0=1.57 g/cm^3, ρ_{0k}=1.61 g/cm^3, D_k=8.33 km/s, and α=0.7. The explosive is initiated in a circle of diameter 6 mm in the center of its free face. The outer surfaces of the system are free boundaries. Our calculations were made for charges whose diameters varied between 10 and 40 mm, their length being equal to 10 diameters.

Table 3 contains the calculated and measured velocities of the detonation wave in PZhV-20U (L is distance to the primer). The measured velocities are averaged over each experimental series.

Table 3. Measured (D_m) and calculated (D_c) detonation velocities in non-sheathed PZhV-20U charges

d=10 mm	L, mm	17-41	41-66	66-95
	D_m, km/s	2.09	1.76	1.78
	D_c, km/s	2.08	1.85	1.76
d=12 mm	L, mm	17-48	48-81	81-113
	D_m, km/s	2.35	1.95	1.90
	D_c, km/s	2.31	2.10	2.08
d=15 mm	L, mm	16-56	56-98	98-145
	D_m, km/s	2.85	2.27	2.30
	D_c, km/s	2.63	2.44	2.42
d=20 mm	L, mm	18-73	73-134	134-194
	D_m, km/s	3.12	2.74	2.72
	D_c, km/s	3.13	2.85	2.85
d=40 mm	L, mm	22-145	145-269	269-390
	D_m, km/s	3.81	3.68	3.64
	D_c, km/s	3.88	3.61	3.61

Table 3 also contains the ranges of L that were used to determine the wave velocity in PZhV-2U. It is seen that calculated results agree well with experiment for all systems and ranges. Velocities for the last two ranges are seen to be almost identical, proving that the process of PZhV-20U detonation has got steady. Figure 3 shows calculated and experimental steady-state detonation velocities as functions of inverse diameter *D(1/d)*. The greatest discrepancy of 9.5% is seen for the 12-mm-diam charge. For both the functions shown in Fig. 3, extrapolation to $d = \infty$ gives D_∞ = (4.0-4.5) km/s.

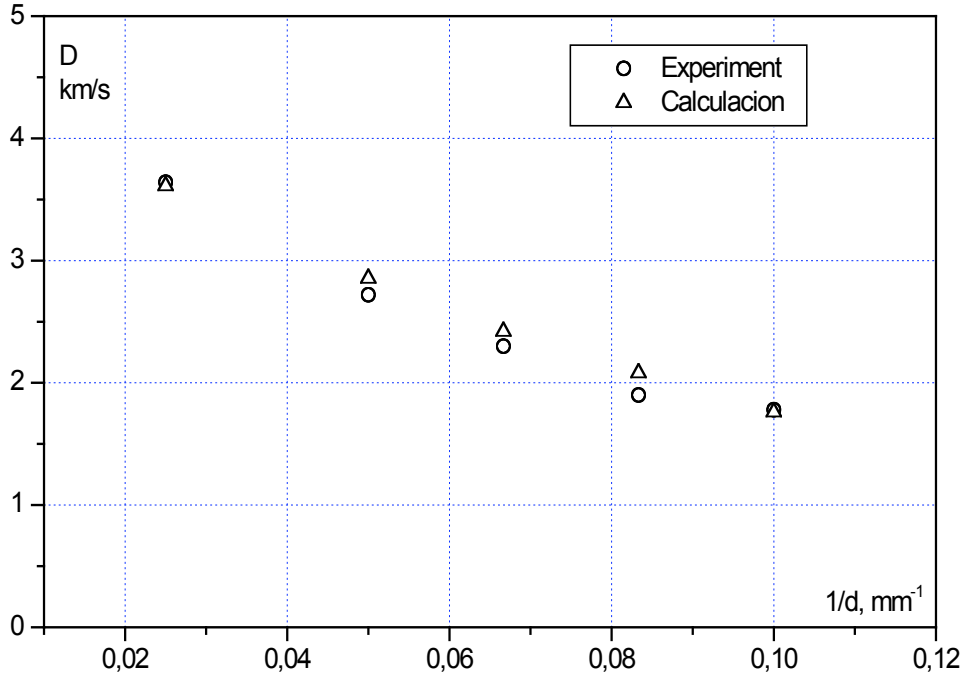

Fig. 3. Detonation velocity vs. diameter

At a distance of several diameters the shape of the detonation front gets steady and does not change at later times. It is almost independent of diameter since the shapes for different diameters are similar to each other. Calculated steady-state pressures and concentrations are shown in Fig. 4.

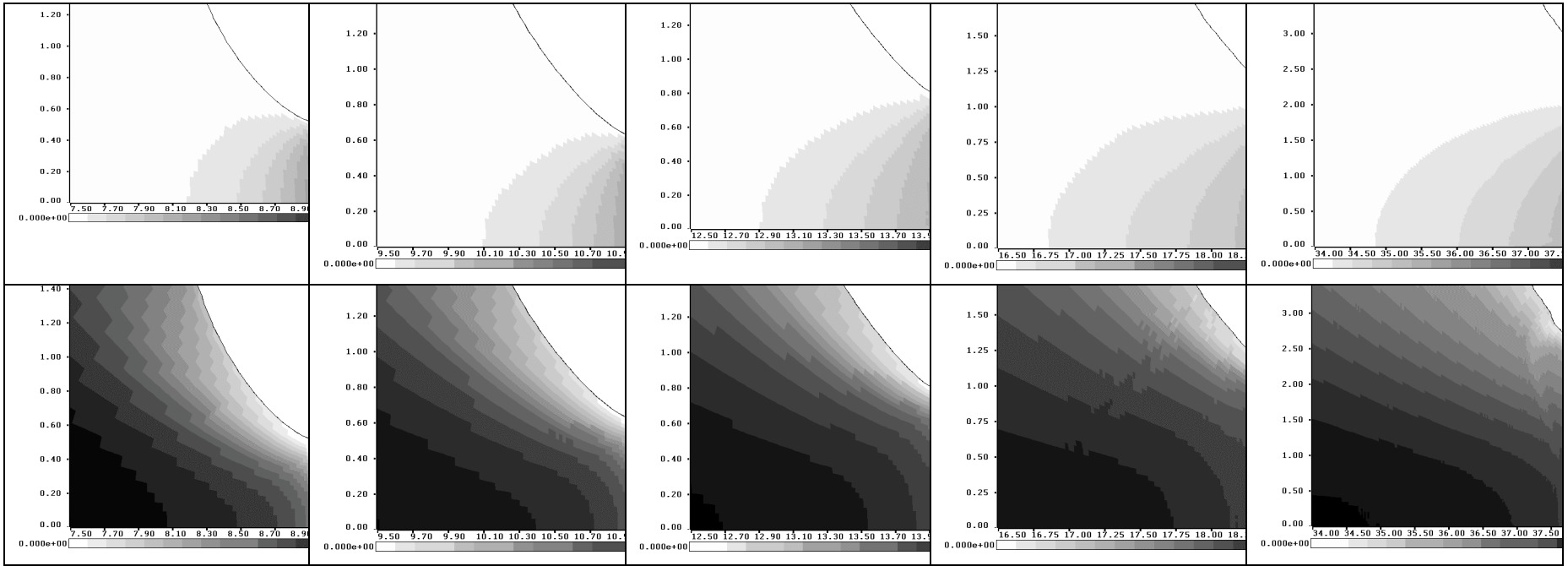

d=10 mm	*d*=12 mm	*d*=15 mm	*d*=20 mm	*d*=40 mm
t=46.0 μ	t=50.0 μs	t=56.0 μs	t=64.0 μs	t=106.0 μs

Fig. 4. Pressures and concentrations.

Table 4 and Figure 4 show calculated data on pressure at the steady-state detonation front as a function of diameter $P_f(d)$. It is seen that the pressure is far from its limiting value for the diameters calculated. Using data from Table 4 and Fig. 5, one can estimate that the critical diameter is $d_{кр}$~15 mm. Table 4 also contains information on PZhV-20U burning which is no greater than 30% in charges of diameters d=10, 12 and 15 mm.

Table 4. Pressure on the wave front and burning for non-sheathed PZhV-20U charges

d, mm	10	12	15	20	40
P_f, GPa	1.52	2.35	3.40	4.50	7.80
$1-\xi$, %	26.0	27.5	30.0	37.0	73.0

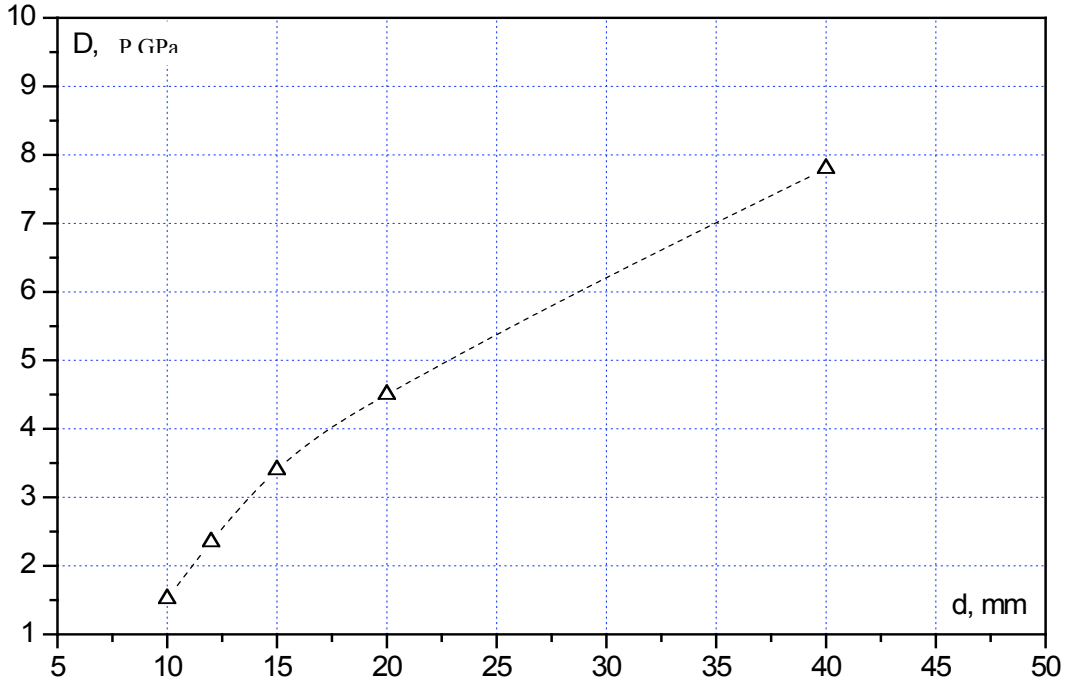

Fig. 5. Calculated pressures on the wave front

The calculated times of detonation wave travel through the PZhV-20U charges of different diameters are shown in Fig. 6 where r is distance from the symmetry axis.

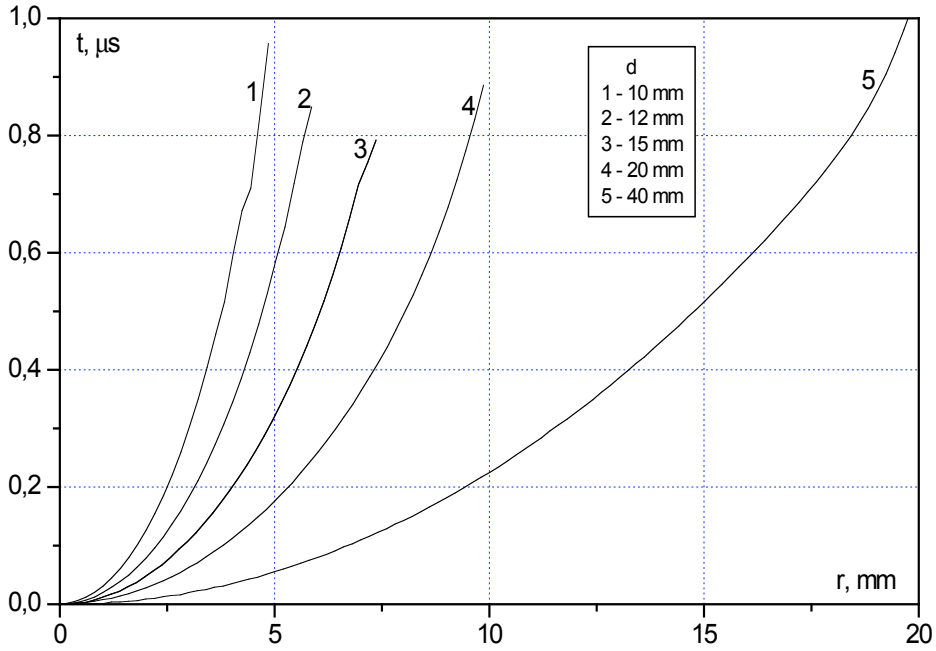

Fig. 6. Wave travel times through PZhV-20U charges

Sheathed charges

Copper-sheathed cylindrical PZhV-20U charges were simulated in a setup corresponding to the actual experimental configuration. The initial geometry is shown in Fig. 7. Primer's parameters are identical to those for non-sheathed charges. The primer was defined to initiate in a 3-mm-diam circle with the center on the symmetry axis. Three calculations for different charge diameters (d=10, 20 and 40 mm) were done. The initial density of the explosive was defined to be ρ_0=1.2 g/cm^3. The sheath was 0.1d thick.

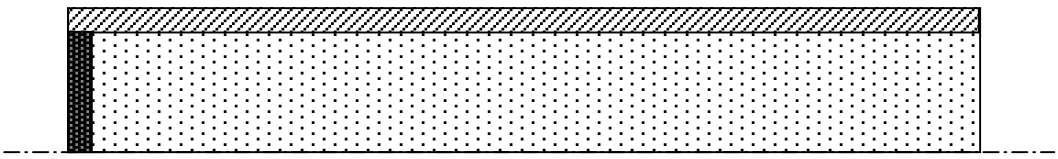

Fig. 7. The sheathed PZhV-20U charge

We calculated velocities and pressures at the front of the steady-state detonation wave. Calculated pressures are shown in Fig. 8. The detonation front is almost flat; its delay at the side relative to the central point makes ~0.015*d*. PZhV-20U burning makes 50%, 68% and 84% for charges of diameters *d*=10, 20 and 40 mm, respectively.

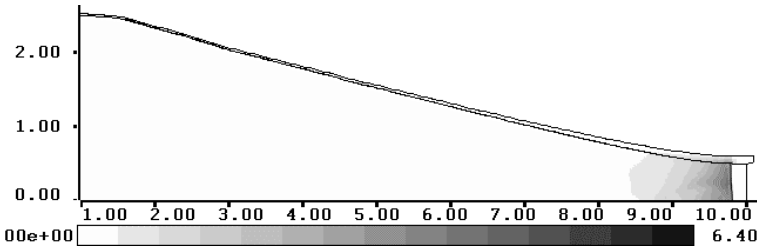

d=10 mm (t=30 μs)

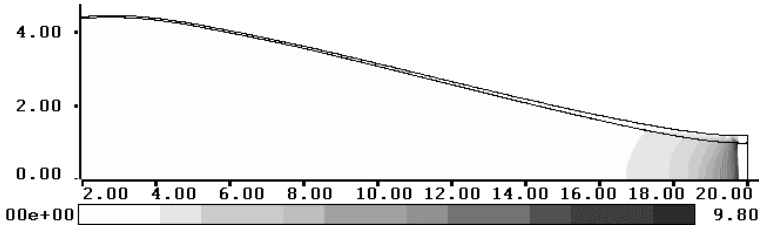

d=20 mm (t=50 μs)

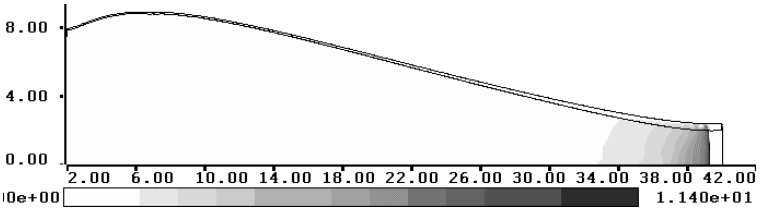

d=40 mm (t=92 μs)

Fig. 8. Calculated pressures in the sheathed PZhV-20U charges

Table 5 compares calculated and experimental results. The charge of diameter d=20 mm shows the greatest difference (7%) between calculated and experimental detonation velocities. Figure 9 shows calculated and experimental detonation velocities as functions of inverse diameter *D(1/d)*. It is seen that as the diameter increases, both the functions tend to D_∞ =(4.7-5.0) km/s that is somewhat higher than the value obtained by extrapolation for non-sheathed charges.

Table 5. Detonation parameters for sheathed PZhV-20U charges

d	$\boldsymbol{D}$, km/s		$\boldsymbol{R_f}$, mm		$\boldsymbol{P_f}$, GPa	
mm	Calculation	Experiment	Calculation	Experiment	Calculation	Experiment
10	3.30	3.28	49	36	6.4	–
20	4.14	3.87	167	122	9.8	6.7*
40	4.48	4.28	357	250	11.4	7.5*

R_f and P_f are, respectively, the radius of curvature and pressure at the detonation front.
* effective Chapman-Jouguet pressure

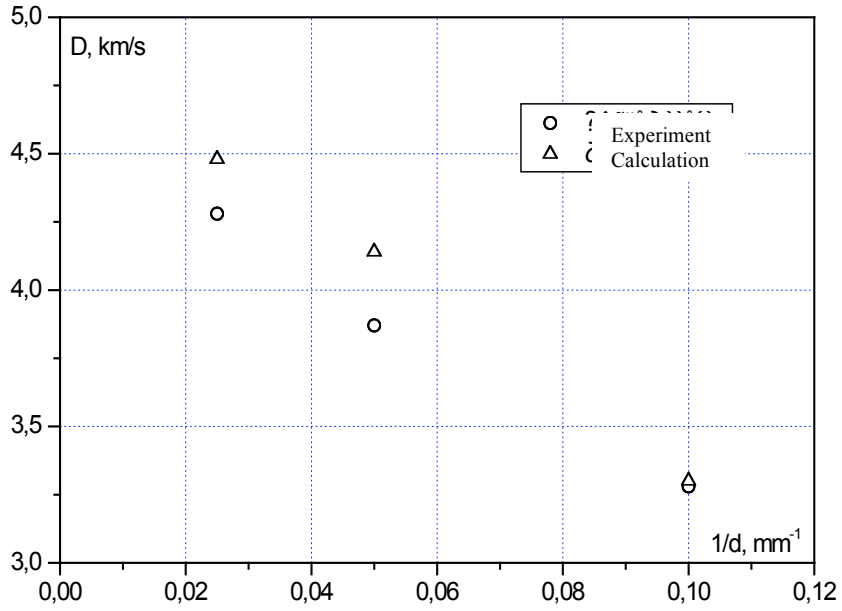

Fig. 9. Detonation velocities for sheathed charges

Figure 10 shows calculated and experimental profiles of the outer surface of the copper sheath. They are seen to agree well. This proves that the equation of state used in our calculations describes the behavior of explosion products rather accurately.

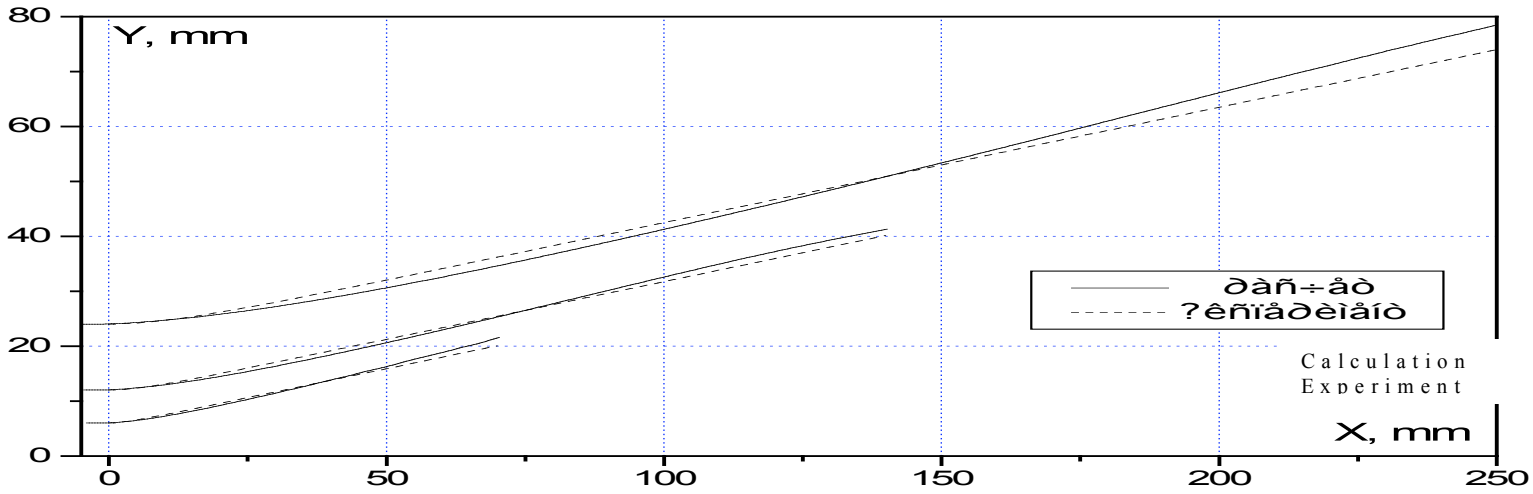

Fig. 10. The outer surface of the copper sheath; PZhV-20U charges of diameters d=10, 20 and 40 mm

Gap-test systems

PZhV-20U sensitivity to shock was studied through gap tests with the divergent initiating wave. We modeled only those where pressure at the front of the shock wave entering the explosive was close to critical. Geometry of our 2D calculations is shown in Fig. 11. A primer (4 mm thick and 60 mm in diameter) initiates from a 3-mm-diam circle. The PZhV-20U charge measures 60 mm in diameter and 20 mm in length; ρ_0=1.2 g/cm^3. A gap of width h between the primer and the PZhV-20U explosive was filled with fluoroplastic. Calculations were done for h=10, 15 and 20 mm.

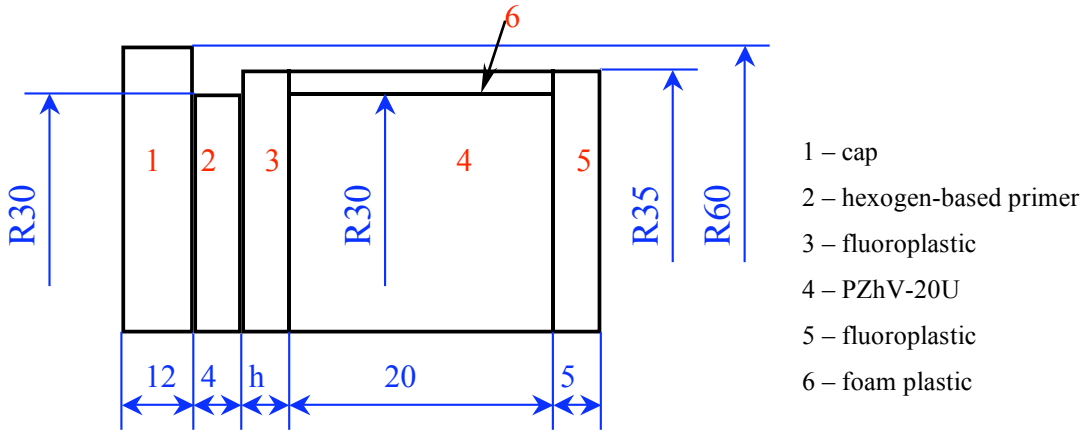

Fig. 11. Gap-test system

Figures 12-14 illustrate the evolution of pressure profiles in these systems (the primer is not shown). It is seen that for h=10 mm and h=15 mm, the normal detonation wave establishes already at a depth of ~8 mm in PZhV-20U, with pressure P_f~8.5 GPa at the front. The shape of the shock front is similar to sphere. In the system where h=20 mm, the detonation conditions are most close to critical, and the normal detonation establishes only in the second half of the PZhV-20U charge (Fig. 14). The shape of the detonation front is more complicated. It is concave in the central part and gets almost flat when the wave exits from the explosive. For the above values of h, the calculated burning at the time of wave exit from the explosive makes ~50%.

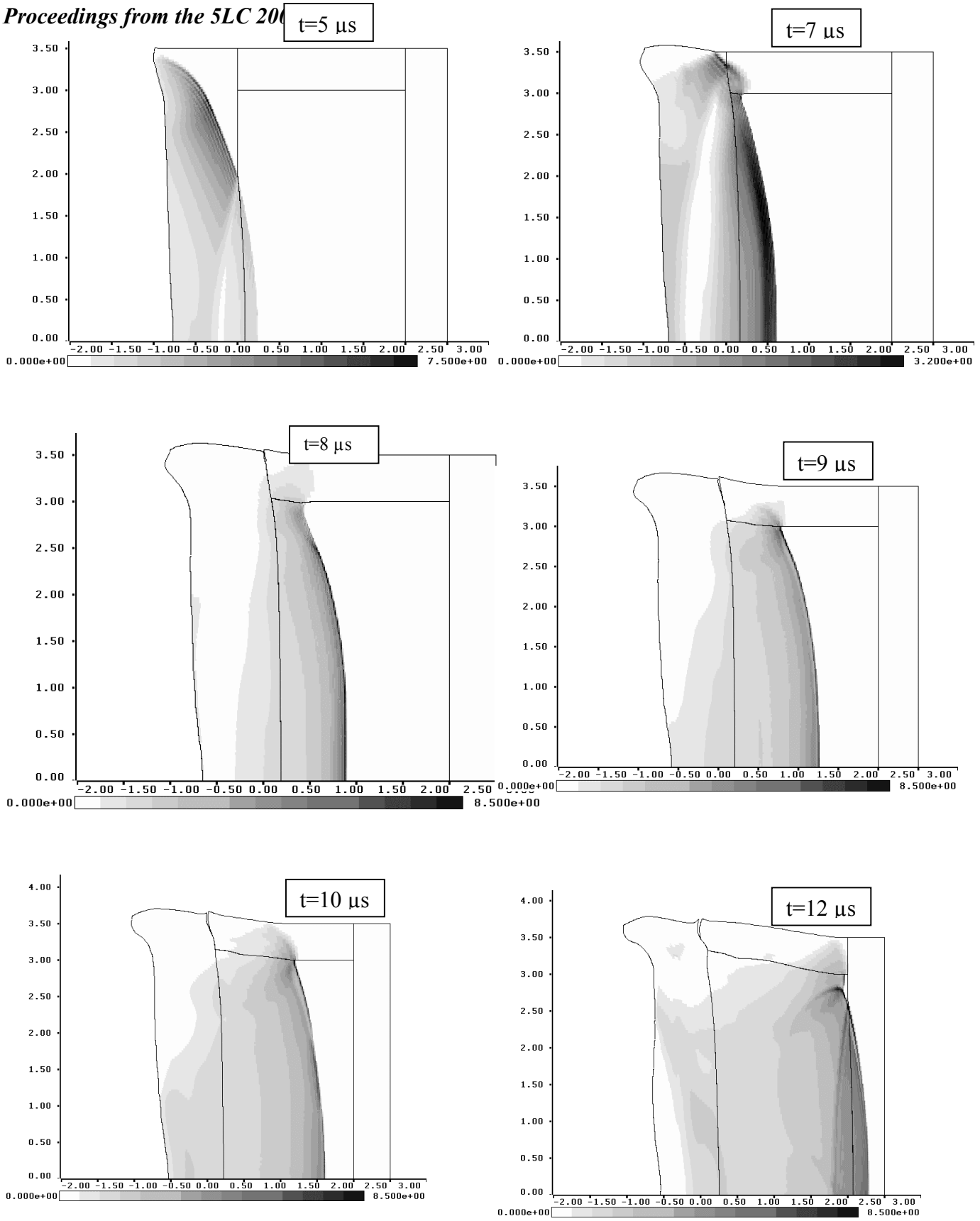

Fig. 12. Calculated pressure profiles for the gap-test system (h=10 mm)

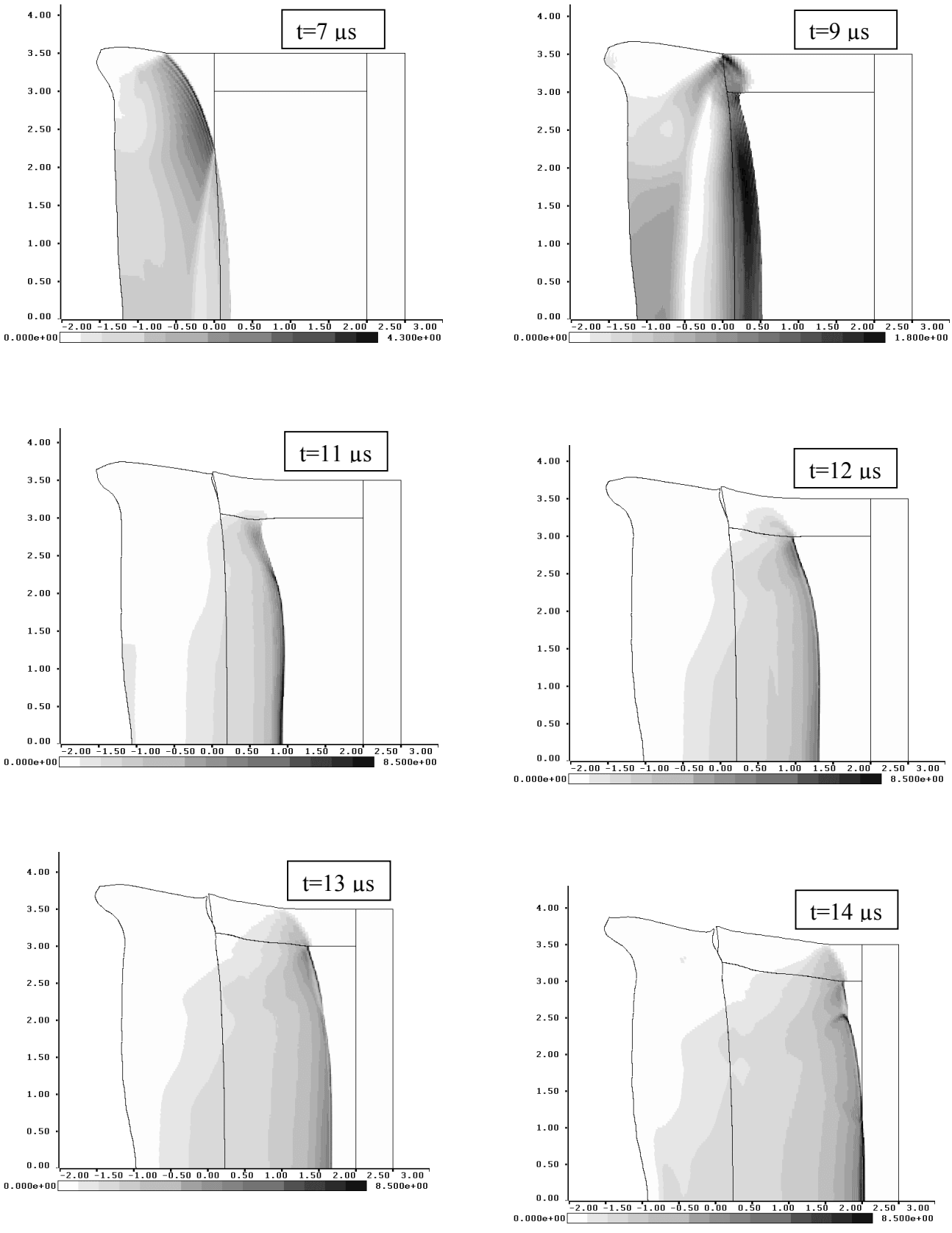

Fig. 13. Calculated pressure profiles for the gap-test system (*h*=15 mm)

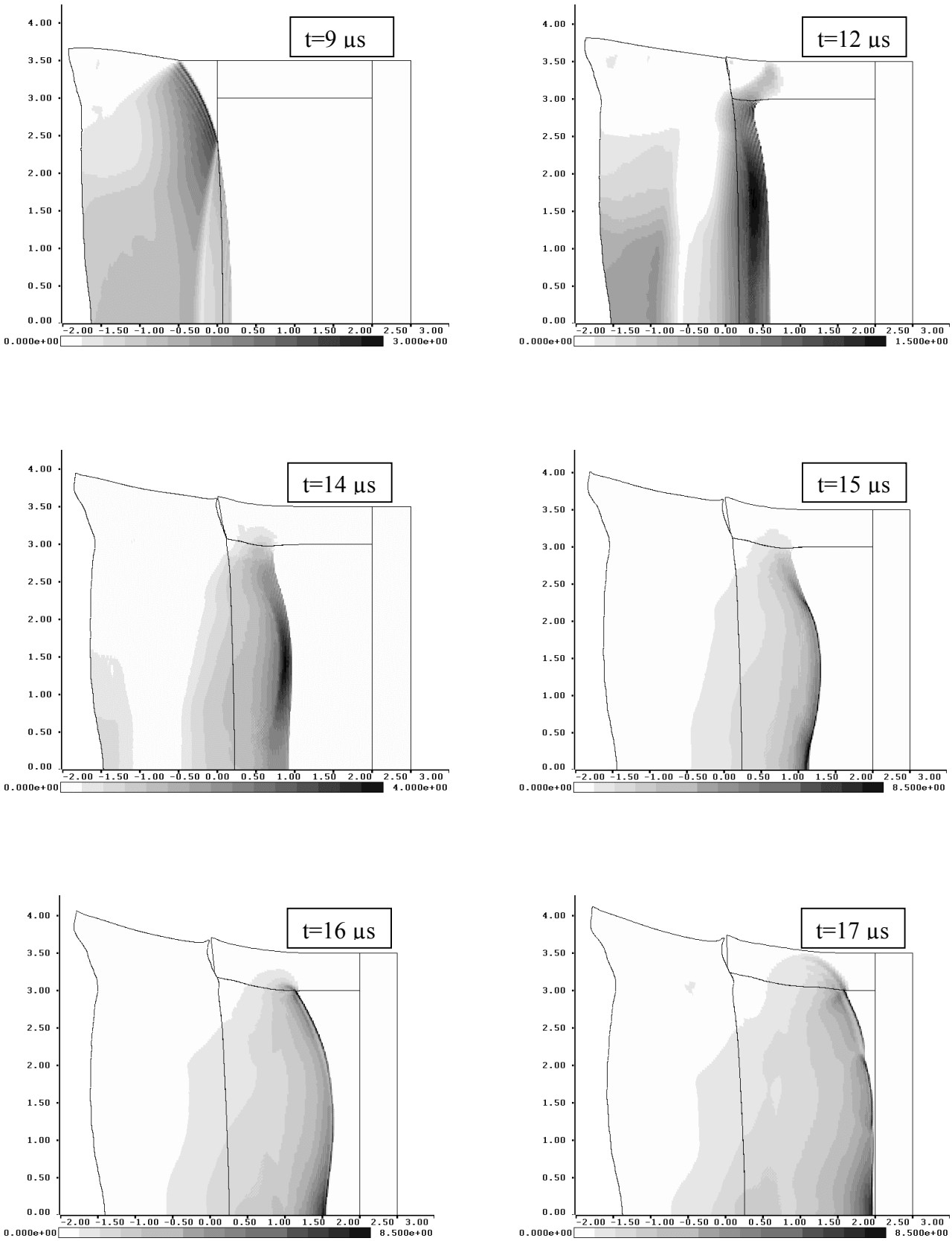

Fig. 14. Calculated pressure profiles for the gap-test system (h=20 mm)

Calculated and experimental shock travel times along the symmetry axis are compared in Table 6 and Fig. 15; they disagree by no more than 3%.

Table 6. Calculated and experimental times of shock travel through PZhV-20U

h, mm	***τ***, μs	
	Calculation	Experiment
10	7.58	7.77
15	8.35	8.48
20	9.46	9.78

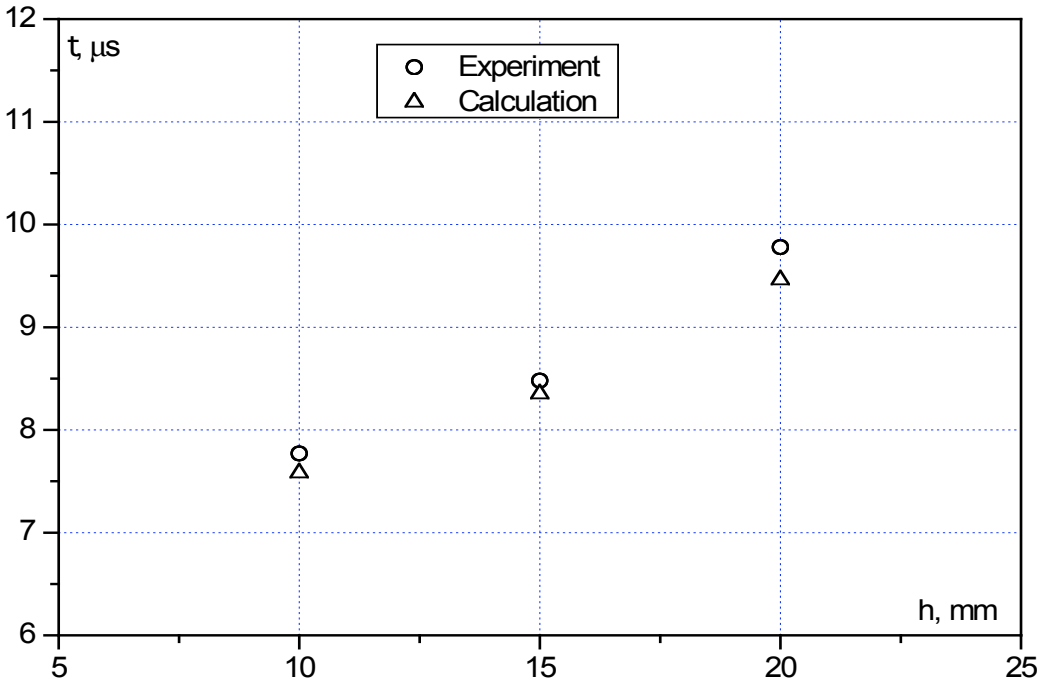

Fig. 15. Calculated and experimental times of shock travel through PZhV-20U

CONCLUSION

2D simulations of experiments with the commercial explosive PZhV-20U showed good agreement between calculated and experimental results on detonation velocity in cylindrical charges of different diameters, both sheathed and non-sheathed, and on PZhV-20U initiation by convergent shocks of different intensity adjusted by the thickness of the gap between the primer and the PZhV-20U charge.

Our calculations rather accurately (within experimental error) reproduce the configuration of the outer surface, observed in experiments for PZhV-20U charges of three diameters (10, 20 and 40 mm) at the final stage of shock propagation, proving, inter alia, that the equation of state used for detonation products is valid.

Our calculations helped obtain the shape of the shock front and detonation parameters for PZhV-20U charges used in different experiments. Calculated and experimental pressure profiles for the steady-state detonation wave in the PZhV-20U explosive agree well.

With appropriate normalization against experimental data, our explosive decomposition model can be used for other explosives.

REFERENCES

1. S.N. Lyubyatinsky, O.V. Kostitsyn, A.A. Nikulin, V.P. Filin, B.G. Loboyko, A.V. Vershinin, and A.B. Syrtsov, Non-ideal PZV-20U explosive knock rating. Abstracts of presentations at the VI Zababakhin Talks, Snezhinsk, 2001, p. 47.
2. N.N. Anuchina, V.I. Volkov, and N.S. Eskov, A numerical method to reconstruct strongly distorted interfaces. Abstracts of presentations at the V Zababakhin Talks, Snezhinsk, 1998, p.131-132.
3. V.F. Kuropatenko, An equation of state for dense explosive detonation products. J. Combustion and Explosion Physics, 1989, V.25, #6, p. 112-117.
4. Y.A. Aminov, A.V. Vershinin, N.S. Eskov et al, A modified model of TATB-based explosive detonation macrokinetics. J. Combustion and Explosion Physics, 1997, V.33, #1, p. 94-97.